

MR Imaging of Motion with Spatial Modulation of Magnetization¹

A novel magnetic resonance imaging technique provides direct imaging of motion by spatially modulating the degree of magnetization prior to imaging. The preimaging pulse sequence consists of a radio-frequency (RF) pulse to produce transverse magnetization, a magnetic field gradient to "wrap" the phase along the direction of the gradient, and a second RF pulse to mix the modulated transverse magnetization with the longitudinal magnetization. The resulting images show periodic stripes due to the modulation. Motion between the time of striping and image formation is directly demonstrated as a corresponding displacement of the stripes. This technique can be used to study heart wall motion, to distinguish slowly moving blood from thrombus, and to study the flow of blood and cerebrospinal fluid.

Index terms: Blood, flow dynamics • Blood, MR studies • Cerebrospinal fluid, flow dynamics • Cerebrospinal fluid, MR studies • Heart, MR studies, 51.1214 • Heart, thrombosis • Magnetic resonance (MR), pulse sequences • Magnetic resonance (MR), technology

Radiology 1989; 171:841-845

THE magnetic resonance (MR) signal has long been known to be sensitive to motion (1,2). One of the principal reasons for motion sensitivity is that when the local magnetization of a material is altered, the material maintains the altered magnetization when it moves (within the limits of the relaxation times). For example, Morse and Singer (3) proposed measuring blood flow by locally altering the magnetization of blood and then detecting the passage of this "tagged" blood downstream. Analogous techniques have been proposed for measurement of blood flow with MR imaging by detecting the passage of blood with locally saturated or inverted magnetization through the region being imaged (4,5). A technique has been proposed (6) for imaging myocardial motion within the plane of the image by using selective excitation to produce a pattern of lines of altered magnetization, the motion of which can be followed. We describe herein a novel technique for producing a spatial pattern of altered magnetization within a region to be imaged, for the purpose of studying motion. We have used this technique to demonstrate myocardial contraction and to distinguish thrombus from slow-moving blood. The technique can also be used to demonstrate the spatial distributions of magnetic field inhomogeneity, radio-frequency (RF) inhomogeneity, and gradient nonlinearity.

MATERIALS AND METHODS

This technique (Appendix) produces a periodic spatial modulation of magnetization (SPAMM) prior to imaging, by using a sequence of two nonselective RF pulses separated by a magnetic-field-gradient pulse (Fig 1). Starting from a condition of uniform longitudinal magnetization (Fig 2a), the first RF pulse turns some of this magnetization (or all, in the case of a 90° flip angle) into transverse magnetization, all initially with the same phase (Fig 2b).

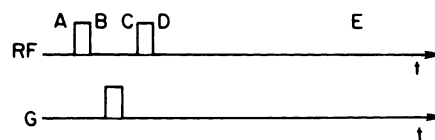


Figure 1. Timing diagram of pulse sequence for SPAMM. RF = radio-frequency excitation, t = time, G = wrap gradient for production of modulation. Letters A-E indicate corresponding times in Figure 2. The time between A and D is assumed to be short relative to the relaxation times.

The gradient pulse produces a periodic spatial modulation of the phase of the transverse magnetization ("wraps" it) along the direction of the gradient (Fig 2c). The second RF pulse mixes the modulated transverse magnetization with the longitudinal magnetization, producing modulated longitudinal magnetization (Fig 2d). Although the second RF pulse need not be identical to the first, if it has the same flip angle, the longitudinal magnetization will be restored to its initial value at the peaks of the modulation. The phase of the second RF pulse is unimportant, except to determine the relative phase of the spatial modulation pattern. An optional second gradient pulse can be used to "spoil" the remaining transverse magnetization. The use of gradients for section selection in the subsequent imaging sequence will also achieve this. The net result is the production of a stack of "planes," or bands, of modulated magnetization.

The SPAMM sequence is analogous to classical two-dimensional MR imaging (7) with its phases of preparation, evolution, and mixing, with the subsequent imaging sequence enabling signal detection. Longitudinal relaxation between production of the bands and imaging will reduce the amplitude of modulation (Fig 2e). The dependence of the amplitude of modulation on the delay between the SPAMM sequence and imaging could be used to estimate the local value of the longitudinal relaxation time, T_1 . The initial amplitude of modulation of the magnetization is de-

Abbreviations: RF = radio frequency, SPAMM = spatial modulation of magnetization.

¹ From the Department of Radiology, Hospital of the University of Pennsylvania, 3400 Spruce St, Philadelphia, PA 19104. Received August 18, 1988; revision requested October 11; revision received January 25, 1989; accepted February 3. L.A. supported in part by the American Heart Association. Address reprint requests to L.A.

© RSNA, 1989

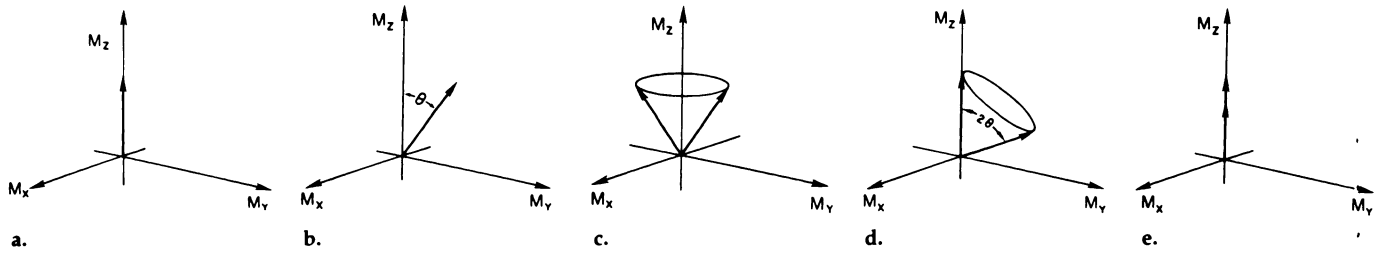


Figure 2. State of magnetization (M) at different times in the pulse sequence in Figure 1. (a) Magnetization prior to initiation of the modulation sequence (time A in Fig 1). Total distribution of magnetization in rotating frame is initially all polarized with value M_0 along the main magnetic field (in the z direction). (b) Magnetization after first RF pulse (time B in Fig 1). RF pulse has flip angle θ , with phase along the x axis in rotating frame. (c) Magnetization after wrap (modulating) gradient pulse (time C in Fig 1). (d) Magnetization after second RF pulse with same values as first (time D in Fig 1). (e) Magnetization after significant relaxation has occurred (time E in Fig 1) and after remnant transverse magnetization has relaxed or been "spoiled."

terminated by the choice of flip angle (eg, a 45° flip angle produces bands of saturation at the troughs, while a 90° flip angle produces bands of inversion). The orientation of the band is determined by the direction of the wrap gradient. The separation of the bands is inversely proportional to the strength and duration of the wrap gradient. For example, a rectangular gradient pulse of 0.6-msec duration and 0.8-G/cm (0.00008-T/cm) amplitude will produce a band spacing of 0.5 cm. The spacing of the bands resulting from a gradient pulse of known shape and duration can be used to calibrate the gradient strength. Chemical shift differences between two regions will produce a relative displacement in the positions of the band patterns. A second set of modulation bands, for example, in a direction orthogonal to the first, can be produced by following the second RF pulse with a second wrap gradient in an appropriate direction and then with a third RF pulse.

In the presence of magnetic field inhomogeneities (effectively creating local gradients), the bands of modulated magnetization may become nonparallel. Keeping the time between the RF pulses short will reduce the evolution of phase modulation due to field inhomogeneity and thus minimize this effect. For studies of cardiac motion, keeping this time short also minimizes the delay between R-wave detection and initiation of imaging.

Nonlinearity of the wrap gradient will also result in nonparallel bands (or varying band spacing, if the nonlinearity is purely one dimensional). However, in this case, decreasing the time between the RF pulses will not reduce the effect. This feature can be viewed as an advantage, rather than a problem, because it can be used to directly display the distribution of gradient nonlinearity. Although most manufacturers correct the reconstructed images for distortions due to gradient nonlinearities, the stripe pattern will still appear distorted in the image, reflecting the actual distorted pattern of the bands in space.

The spatial modulation of the longitudinal magnetization is made visible by the resulting modulation of the transverse magnetization in the subsequent imaging pulse sequence, which appears as stripes with sinusoidal variation of in-

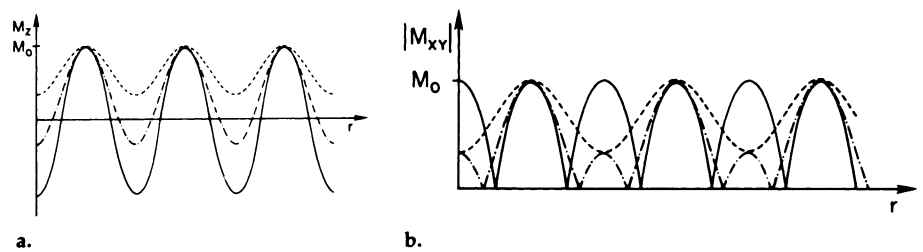


Figure 3. Magnitude of transverse magnetization, M_{xy} (proportional to image intensity), along direction of wrap gradient, r , resulting from imaging of modulated longitudinal magnetization, M_z . (a) Different degrees of modulation of M_z , ranging from full inversion in troughs (solid line) to partial saturation (dashed line). (b) Corresponding resulting $|M_{xy}|$. The different initial states could reflect different flip angles or different degrees of relaxation after an initial inverting modulation.

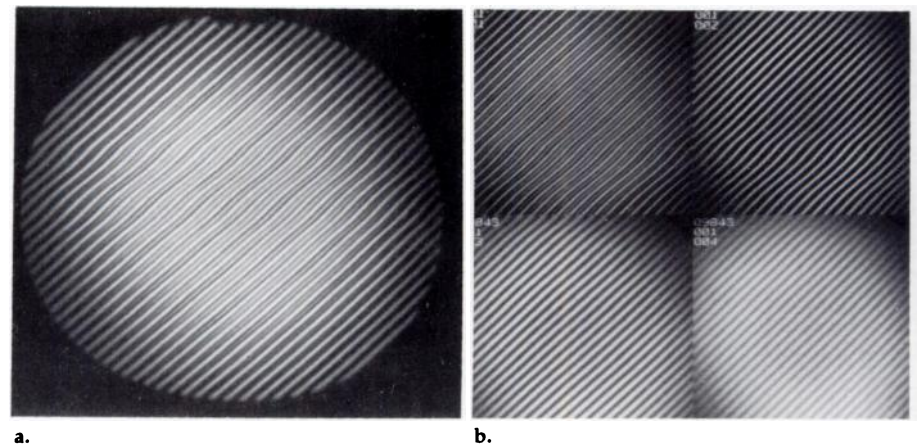
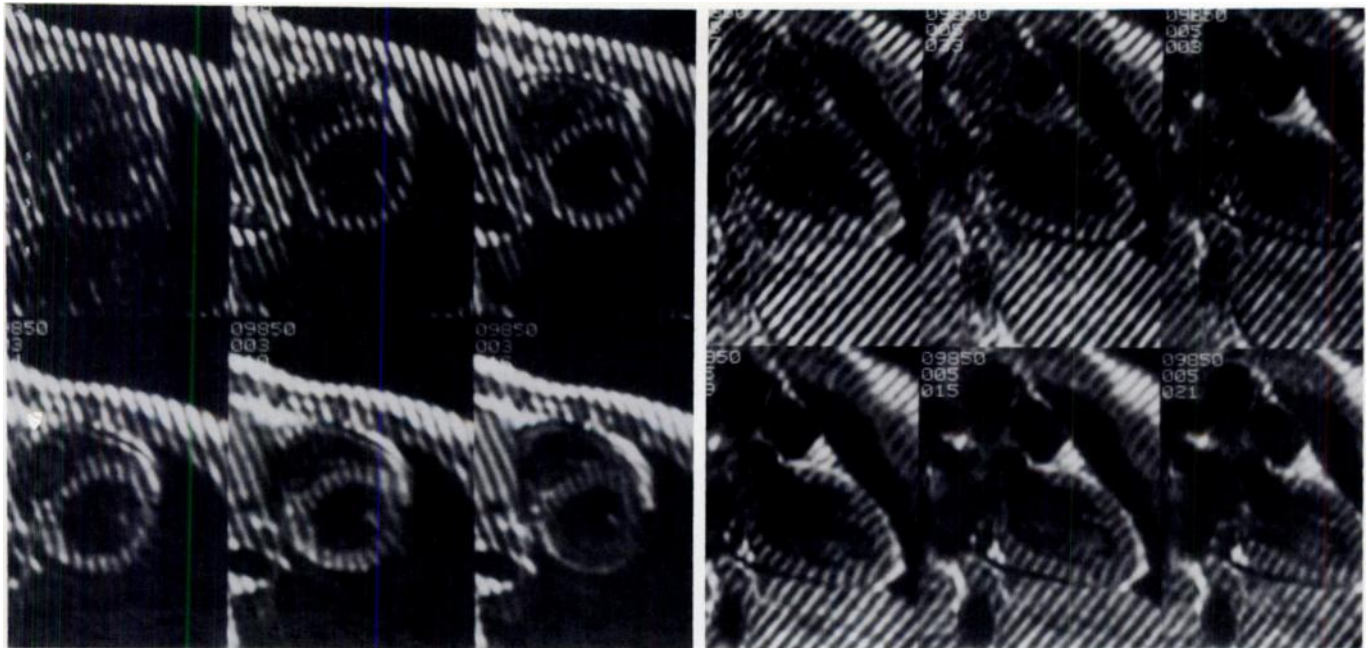


Figure 4. Images of a 28-cm-diameter cylindrical phantom filled with copper sulfate solution, obtained after SPAMM sequence with 90° RF flip angles, producing inversion in troughs of modulation. (a) Image obtained 3 msec after SPAMM sequence. Notice pairwise convergence of stripes peripherally, due to RF inhomogeneity. (b) Series of images with 45-msec incremental increases in delay between SPAMM and imaging, from top left (image in Fig 4a) to top right to bottom left to bottom right. Note initial pairwise merging of stripes, followed by fading of stripes without further motion.

tensity in the image. Phase alternation of the refocusing RF pulses in the imaging sequence can help prevent artifacts due to stimulated echoes. The stripes correspond to the intersection of the bands of modulation and the imaged section.

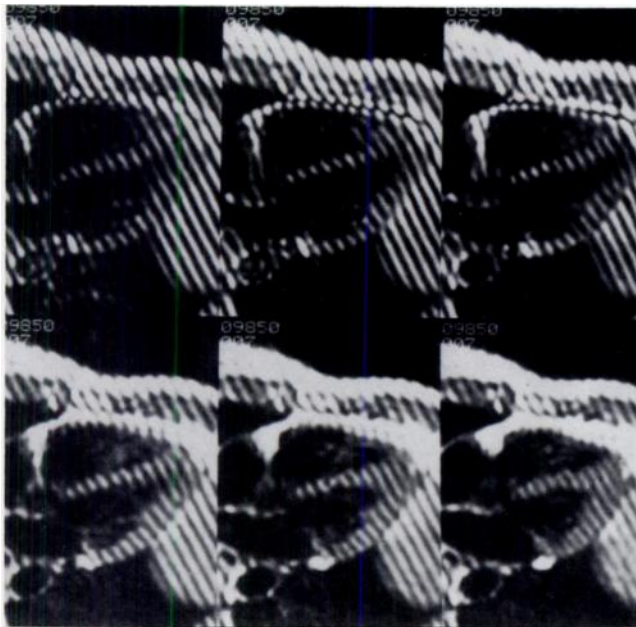
Most MR imaging systems display the magnitude but not the sign of the magnetization. Therefore, if the SPAMM sequence produces inversion of the magnetization (ie, RF flip angle greater than

45°), intensity minima will be seen in the image at points where the longitudinal magnetization crosses through zero immediately prior to imaging (Fig 3). Thus, for modulation with inversion of magnetization, there will be twice as many stripes in the resulting image as there would be for modulation with only saturation. With increasing delay between the SPAMM sequence and imaging, longitudinal relaxation will result in the pair-



a.

b.



c.

Figure 5. Images of a healthy 30-year-old woman, acquired with a cardiac-gated SPAMM imaging sequence in three orthogonal planes with an echo time of 20 msec. The subject's heart rate was 56 beats per minute. Images are displayed with incremental 45-msec increases in delay between SPAMM sequence and imaging, as in Figure 4b.

(a) Short-axis view through ventricles.
 (b) Long-axis view through left ventricle.
 (c) Four-chamber view through ventricles.

at a rate determined by the local T1 relaxation times (as it is the modulation of the longitudinal magnetization that produces the stripes). In moving tissue, the stripes will move with the tissue. The displacement of the stripes indicates the corresponding amount of motion at right angles to the stripes between the time of tissue labeling with SPAMM and subsequent signal detection with imaging. The positions of the stripes in surrounding stationary tissues provide a convenient visual reference for assessing motion. More precise measurements of motion can be made by comparing the image with one made immediately after labeling. If there is danger of aliasing due to motion greater than the interstripe distance, either the stripe spacing can be increased by decreasing the wrap gradient (amplitude or duration) or additional images can be made at intermediate times when less motion has occurred. In the case of more complex motions, moving the object through the imaging plane, the degree of such motion can be assessed by acquiring an orthogonal set of images with stripes corresponding to the orientation of the original image plane, to permit correction for such "pull-through" effects. Because the stripes are formed by an intersection of the modulated bands with the section, if the object rotates through the imaging plane, the obliqueness of the intersection may decrease the visibility of the stripes. This effect can be minimized by minimizing the section thickness.

The SPAMM sequence in Figure 1 was implemented on a conventional commercial 1.5-T MR imaging system (Signa; GE Medical Systems, Milwaukee). In practice, a separate spoil pulse is unnecessary, because the imaging gradients will perform that function. A conventional cardiac-gated imaging sequence has been modified by adding the SPAMM sequence prior to imaging. The total duration of the sequence is less than 3 msec, adding a mini-

wise merging of the stripes at a time when the magnetization in the troughs equals zero. Further delays will result in fading of the stripes but no further movement (for stationary tissue). The time of merging of the stripes with initial inversion modulation can be used to estimate the value of the local T1 relaxation time, in a manner analogous to the use of T null in classic inversion-recovery measurements of T1 (8).

In the case of RF strength (B_1) inhomogeneity, the degree of inversion will correspondingly vary across the image. This variation will be reflected in varying spacing between the pairs of stripes if inversion has been produced in the modulation, providing a means of demonstrating the RF inhomogeneity independent of image intensity. If only saturation is produced in the modulation, the position

of the stripes is independent of RF strength, making this technique insensitive to RF variation when used for studying motion.

Due to longitudinal relaxation, the stripes produced by modulation with saturation at the troughs will not persist as long as those produced by inversion. However, if, for instance, one wishes to study the diastolic phase in a subject with a slow heart rate, a delay could be introduced between R-wave detection and the SPAMM sequence (eg, at the end of systole).

In stationary tissue, the stripes will remain stationary with different delays between SPAMM and imaging, except for the merging of pairs of stripes described above for modulation that produces inversion. With increasing delays, the stripes will fade (assuming no inversion)

mal delay to the initiation of imaging after R-wave detection. The SPAMM sequence only minimally increases the RF dose of the imaging sequence.

RESULTS

Images of a cylindrical phantom, obtained with a 90° RF flip angle in the SPAMM sequence (producing inversion), are shown in Figure 4 for a series of increasing delays between modulation and imaging. Representative cardiac-gated images from a multiplanar, multiphase study of a healthy volunteer are shown in Figure 5 (informed consent was obtained).

Images of a patient with mitral stenosis and strong echocardiographic indications of intraatrial thrombus are shown in Figure 6. Conventional MR imaging disclosed high signal intensity in the left atrium, suggesting thrombus. However, no stationary stripes were seen on the SPAMM images, indicating that it was all slow-moving blood and not thrombus. At surgery for mitral valvuloplasty, there was no thrombus in the atrium.

Images of blood vessels show displacement of the stripes within the lumen, corresponding to motion of the blood between labeling by the SPAMM sequence and imaging. With turbulence or rapid flow, shearing of the stripes within the section being imaged can cause disappearance of the stripes with increasing delays between SPAMM and imaging, even though the flow may be too slow to affect the underlying blood signal.

The application of SPAMM to the study of the motion of cerebrospinal fluid is shown in Figure 7. There was a clear difference in the amount of motion above and below the level of a tumor with epidural extension, corresponding to tumor block of the flow of cerebrospinal fluid.

DISCUSSION

The primary function of the heart is contraction, and it is to be expected that diseases of the heart, such as ischemia and infarction, would generally result in altered contraction patterns. The direct demonstration of the contraction of cardiac muscle has previously been difficult. Most imaging techniques show only the inner or outer surfaces of the heart, not the motion of the muscle itself. For example, simple fluoroscopy or kymography shows motion of the outline of a projected cardiac silhouette. Studies performed after intravascular admin-

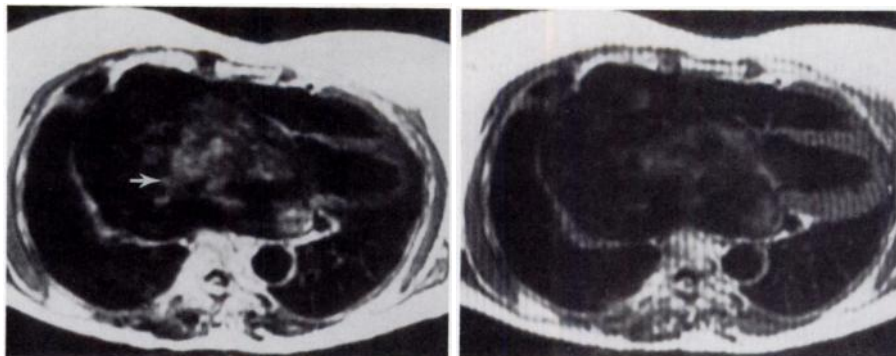


Figure 6. Cardiac-gated images (echo time of 20 msec) of a 63-year-old woman with mitral stenosis. The heart rate was approximately 84 beats per minute, with the patient in atrial fibrillation. (a) Representative conventional image at the level of the left atrium obtained 276 msec after the R wave shows relatively high signal intensity in the left atrial cavity (arrow). (b) Image at the same level and with the same timing as in a but with SPAMM sequence. Notice stripes in stationary structures and heart wall, but not within the left atrium.

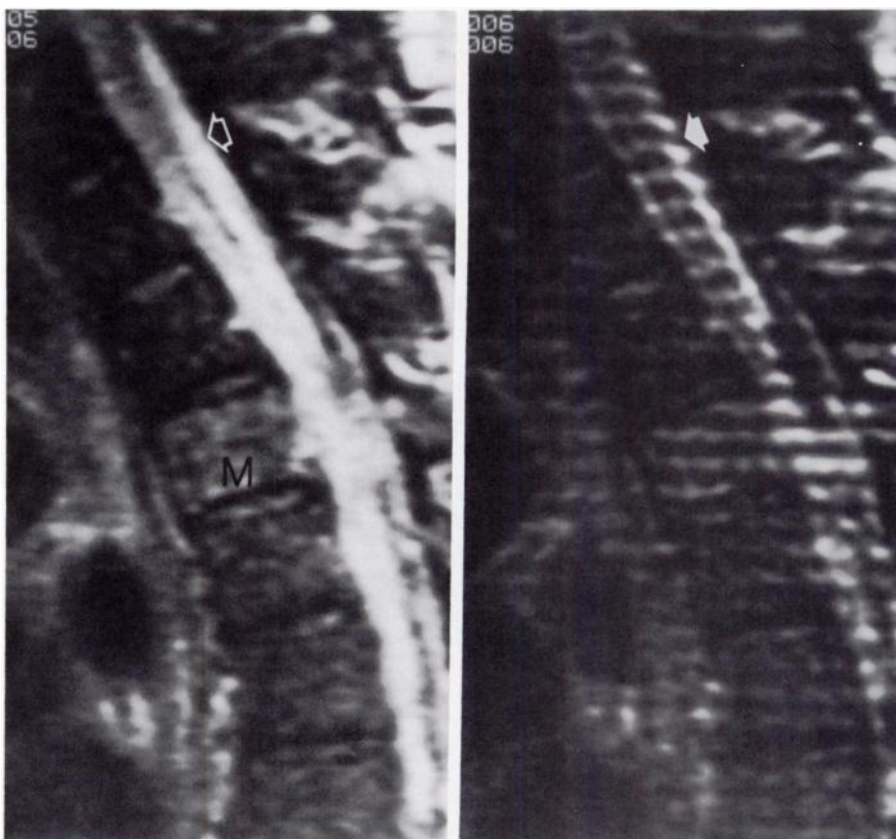


Figure 7. Cardiac-gated surface-coil sagittal images (repetition time = 2,770 msec, echo time = 70 msec) obtained 182 msec after the R wave in a patient with metastasis at T-4 with epidural extension. (a) Conventional image shows relatively increased signal intensity from metastasis (M) and cerebrospinal fluid (arrow). (b) Image at the same level and timing as a but with SPAMM sequence (5-mm stripe spacing). Note downward displacement of stripes above tumor due to motion of cerebrospinal fluid (arrow).

istration of contrast medium and after radionuclide-labeled red blood cell studies show only motion of the endocardial surface. Conventional MR imaging and computed tomography can show the wall thickness but not motion within the wall. Invasive placement of radiopaque markers,

such as beads or screws, or ultrasound transducers permits tracking of actual fixed points on the heart wall. However, the sampling of these points is still relatively coarse, and the distribution of motion between them (eg, transmurally) is still not well defined.

In contrast to these older techniques, MR imaging with magnetic labeling of the myocardium permits a direct demonstration of myocardial motion across the thickness of the wall and at many effective locations. Both absolute and relative motions of the heart can be measured. The particular technique for myocardial labeling presented here is flexible, fast, and easy to use and allows labeling of large regions. Although we could alternatively use tailored RF pulses to excite selectively (for saturation or inversion) particular "planes" through the region to be imaged, the labeling of multiple planes requires either large RF power in one or a few pulses or a series of pulses, which may take a relatively long time. This limitation has two potentially bad consequences: It increases the delay after the R wave before data can be obtained, and it may introduce significant differences in the times at which different planes are labeled, potentially complicating the analysis. One relative advantage of the selective-excitation technique for labeling is that relatively sharply defined bands can be produced, while the SPAMM technique produces sinusoidal profiles of the labeled bands.

One problem that has affected all tomographic studies of heart wall motion is that the motion of the heart through the fixed planes of imaging can result in apparent motion and thickening of a region simply due to the geometric effect of tangentially cutting through the curved surfaces of the heart wall in a more peripheral location as the heart is pulled through the imaging plane. Thus, study of myocardial motion must involve three-dimensional analysis to correct for such pull-through effects. Suitable orthogonal sets of striped images can provide the data needed for such an analysis. Also, although pull-through effects may change the apparent thickness of the heart wall, they will not change the spacing of the stripes, permitting pull-through effects to be distinguished from true contraction even on a single set of images. Although it is straightforward to produce a two-dimensional array of stripes with SPAMM, their sinusoidal profiles result in an overall decrease in the signal-to-noise ratio of the image and make it more difficult to appreciate the underlying anatomy.

The other principal motion effect in MR imaging is the production of phase shifts in excited spins moving along magnetic-field gradients. Thus,

images that display the phase of the signal have been used to demonstrate effects from cardiac motion, as well as blood flow (9). Although the phase images may look superficially similar to SPAMM images, particularly when a strong phase shift is induced across the image by shifting the center of the echo relative to the data acquisition window (10), the physics are rather different. One potential problem in analysis of such images is in calculating displacement from the phase, because the phase shift will generally depend not only on velocity but also on acceleration and other higher-order variables. Other potential sources of phase shift must also be corrected for in calculating displacement.

In summary, SPAMM provides a simple and effective way to demonstrate cardiac motion directly. It also is useful in studying the flow of blood or cerebrospinal fluid and in distinguishing slow-flowing blood from thrombus. Adaptation of the technique will permit a wide range of other applications, including demonstration of the distribution of magnetic field and RF field inhomogeneities and gradient nonlinearities, measurement of T1, calibration of gradients, and demonstration of chemical shift differences. ■

Acknowledgments: We acknowledge the many helpful discussions with our colleagues, including Nathaniel Reichek, MD, Eric Hoffman, PhD, and John Listerud, MD, PhD.

APPENDIX

The fundamental equation is the Larmor relationship between the resonance frequency ω and the magnetic field B : $\omega = \gamma B$, where γ , the proportionality constant, is the gyromagnetic ratio. The magnetic field experienced by a nucleus at a position r is given by the sum of the main magnetic field $B_0(r)$ and any applied magnetic-field gradients. In the case of linear gradient fields and a homogeneous main field, we can write $B(r) = B_0 + Gr$, where G is the component of the gradient along the direction of r .

Chemical shift effects can produce a further change in effective magnetic field B_{eff} for example, between fat and water, in accordance with the equation $B_{\text{eff}} = B(1 - \sigma)$, where the difference in the chemical shift parameter σ is on the order of 3 ppm for fat and water.

The MR signal is detected relative to a reference frequency, typically set equal to that of water in the average main field. The phase φ of the transverse magnetization will evolve in time at a rate dependent on the difference between the local resonance frequency and the reference frequency. In the absence of chemical

shift effects, for a uniform main field with the reference tuned to the resonance frequency and linear gradients, the gradients will cause the phase to evolve as follows: $\varphi(r) = \gamma \int G(t) r dt$, where $t = \text{time}$. This corresponds to a sinusoidal modulation of the x and y components of the transverse magnetization (with a 90° phase shift between them) along the direction of the applied gradient, with a spatial wavelength R of $2\pi / \gamma \int G(t) dt$. Thus, the spacing of the final stripes will depend inversely on the integral of the gradient pulse. If there are nonlinearities of the gradients, as may be found toward the ends of the magnet, the spacing of the stripes will change correspondingly, with the stripes flaring out as the gradients become weaker.

If two regions have chemical shift variables differing by $\Delta\sigma$, the stripes will have the same spacing in each region, but the patterns will be offset from each other by a distance d given by the equation $d = \gamma B_0 \Delta t \Delta\sigma$, where Δt is the time between the two RF pulses. Similarly, in the presence of magnetic field inhomogeneity $\Delta B(r)$, arising either from imperfections in the magnet or from the object being imaged (eg, due to regional susceptibility variations), there will be a corresponding local phase offset at the time of the second RF pulse of $\Delta\varphi(r) = \gamma \Delta B(r) \Delta t$. This will cause the stripes to deviate from parallel. Both of these effects can be minimized by keeping Δt short.

References

1. Hahn EL. Spin echoes. *Phys Rev* 1950; 80:580-594.
2. Suryan G. Nuclear resonance in flowing liquids. *Proc Indian Acad Sci [A]* 1951; 33:107-111.
3. Morse OC, Singer JR. Blood velocity measurements in intact subjects. *Science* 1970; 190:440-441.
4. Axel L. Approaches to nuclear magnetic resonance imaging of blood flow. *Proc SPIE* 1982; 347:336-341.
5. Singer JR, Crooks LE. Nuclear magnetic resonance blood flow measurements in the human brain. *Science* 1983; 221:654-656.
6. Zerhouni E, Parrish D, Rogers WJ, Yang A, Shapiro EP. Human heart: tagging with MR imaging—a method for noninvasive measurement of myocardial motion. *Radiology* 1988; 169:59-64.
7. Aue WP, Bartholdi E, Ernst RR. Two-dimensional spectroscopy: application to nuclear magnetic resonance. *J Chem Phys* 1976; 64:2229-2246.
8. Farrar TC, Becker ED. *Pulse and Fourier transform NMR*. New York: Academic Press, 1971.
9. Van Dijk P. Direct cardiac NMR imaging of heart wall and blood flow velocity. *J Comput Assist Tomogr* 1984; 8:429-436.
10. Wedeen VJ, Rosen BR, Chesler D, Brady TJ. MR velocity imaging by phase display. *J Comput Assist Tomogr* 1985; 9:530-536.